Journal of the Korean Physical Society, Vol. 49, No. 2, August 2006, pp. 577∼584

Guided Mode Propagations of Grounded Double-Positive and Double-Negative Metamaterial Slabs with Arbitrary Material Indexes

Ki Young Kim,* Young Ki Cho and Heung-Sik Tae
School of Electrical Engineering and Computer Science, Kyungpook National University, Daegu 702-701

Jeong-Hae Lee
Department of Radio Science and Communication Engineering, Hongik University, Seoul 121-791

(Received 13 February 2006, in final form 18 May 2006)

The guided dispersion characteristics of grounded slab waveguides whose permittivities and permeabilities are simultaneously negative are numerically investigated. Several different sets of materials with simultaneously negative permittivities and permeabilities are chosen in order to clarify the effects of the material constants on the guided dispersion characteristics. The dispersion characteristics of grounded double-negative slab waveguides are also compared with those of their double-positive counterparts. For the grounded double-negative metamaterial slab waveguides, superslow waves, backward waves, and mode suppressions are observed in certain circumstances, which cannot occur in conventional grounded dielectric slab waveguides. The present results may find applications in the areas of compact waveguiding structures using subwavelength guidance.

PACS numbers: 71.36.+c, 42.25.Bs, 84.40.Az
Keywords: Backward wave, Double-negative index, Grounded slab waveguide, Guided dispersions, Metamaterial, Negative group velocity, Surface polariton.

I. INTRODUCTION

In the 1950's and the 1960's, there was tremendous interest in producing artificial dielectrics with arbitrary values of the permittivity by inclusion of metal particles or wires in the host (natural) dielectric medium. (See Ref. 1 and references therein.) Among the several applications of the artificial dielectrics were microwave / millimeter wave leaky wave antennas [2], where the effective dielectric constants were between zero and unity. Since the dielectric constants of the artificial dielectrics composing novel leaky wave antennas could not be attained in nature, the characteristics of the leaky waves were unique in comparison with those of ordinary leaky wave antennas.

In the late 1990's, attempts to attain even negative permittivity by using metallic wires in the GHz band were made by Pendry *et al.* [3], which was similar, in principle, to the plasmons of metals in optical frequency regions. Pendry *et al.* also suggested that an effective negative permeability could be attained in the GHz band from a periodic arrangement of split ring resonators (SRRs) [4]. Based on Pendry's exceptional ideas on artificially controllable permittivities and permeabilities of media, in the year 2000, Smith *et al.* assembled metallic wires and SRRs to create simultaneously negative permittivity and permeability in the same desired frequency range [5]. Interestingly, this currently well-accepted idea originally dates back to the 1960's. A Russian physicist, V. G. Veselago, theoretically predicted several extraordinary electromagnetic phenomena of materials with simultaneously negative permittivities and permeabilities [6], which were a sign change of group velocity, reversals of the Doppler and the Vavilov-Cerenkov effects, negative refraction, perfect lensing, and a reversal of radiation pressure to radiation tension. However, his ideas were forgotten until the experimental verification was made by Smith *et al.*, because these exotic materials were thought not to exist in nature at all. This experimental verification of simultaneously negative permittivity and permeability ignited the present explosive research worldwide in various phases for both fundamental electromagnetic phenomena and practical applications of these unusual materials in various frequency ranges from radio to optical frequencies. (See recent review papers [7, 8] and references therein.)

Usually, these materials are called metamaterials (MTMs). Although the term MTM has not been strictly defined yet, it is generally admitted to refer to an artificially designed electromagnetic structure with unusual electromagnetic properties that are rarely found in nature. "$Meta-$" is a Greek prefix meaning "*beyond*," so MTMs can be understood as materials that exhibit an

*E-mail: doors@ee.knu.ac.kr; Phone: +82-53-950-5536

extraordinary electromagnetic response. In the MTMs, the directions of the electric field ($\vec{E}$), the magnetic field ($\vec{H}$), and the wave propagation vector ($\vec{k}$) obey the left-hand rule instead of the right-hand rule in ordinary dielectric materials, so MTMs are also commonly referred to as left-handed (meta)materials (LHMs). The reversals of the phase and the energy propagations in MTMs due to the left-handedness lead to backward wave (BW) propagations with opposite directions of the phase and the group velocities, *i.e.*, negative phase velocity (NPV) or negative group velocity (NGV). Thus, the terms BW-, NPV-, and NGV-media are also used for MTMs. Since refraction is reversed when electromagnetic waves are incident on MTMs, they are also called materials with negative refractive index (NRI) or negative index media (NIM). As above, MTMs are media with simultaneous negative permittivity and permeability at a given frequency, so MTMs are also called double-negative (DNG) media.

Due to the DNG property, the electromagnetic wave propagations along these exotic media are quite extraordinary, as above. As such, surface waves at the interface between the DNG media and conventional dielectric media [9] also differ in their propagation behaviors from those at the interface between two dissimilar conventional dielectric media. For example, slab waveguides with DNG media also have extraordinary guided dispersion characteristics [10–13].

In this paper, we investigate the guided dispersion characteristics of grounded slab waveguide structures which have been widely used in the area of microwave and millimeter wave circuits and antennas. For this purpose, the grounded slabs to be analyzed here are of two types, *i.e.*, grounded DNG and DPS[1] slabs. The guided and the leaky dispersion characteristics of the grounded DNG slab waveguides have been studied by several independent groups [14–17]. Baccarelli *et al.* studied the existence of proper guided mode solutions [14,15], as well as the characteristics of the leaky modes [15]. Li *et al.* investigated the guided complex wave solutions [16], and Mahmoud and Viitanen studied surface wave characteristics with emphasis on their power-carrying characteristics [17]. However, the previous results on the guided dispersion characteristics of grounded MTM slab waveguides have been mostly limited to dispersion analyses with fixed specific material parameters of permittivity and permeability. Thus, the roles of both material constants on the guided mode dispersions of the waveguides with MTM inclusions do not seem to have been elucidated exhaustively. Accordingly, we concentrate on the effects of the material parameters on the guided dispersion characteristics of the grounded MTM slab waveguides by introducing several sets of positive and negative permittivity and permeability with their products kept constant. A comparative study was also done between grounded DPS and DNG slab waveguides. Several new findings, which are associated with the effects of the material constants, were observed and discussed in Section III, based upon the qualitative descriptions of the grounded MTM slab waveguides in Section II.

[1] Double-positive, *i.e.*, simultaneously positive permittivity and permeability.

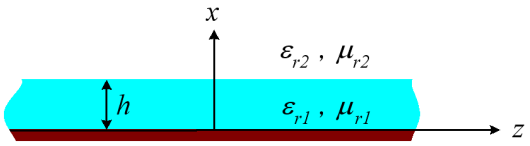

Fig. 1. Schematic illustration of a grounded slab waveguide. The relative permittivity and permeability of the slab can be either those of a DPS or DNG medium.

Table 1. Combinations of ε_{r1} and μ_{r1} of the DPS (+) and the DNG (–) MTMs in the present study. The product values are always kept the same, *i.e.*, $\mu_{r1}\varepsilon_{r1} = +4.0$.

	ε_{r1}	μ_{r1}
a	± 8.0	± 0.5
b	± 5.0	± 0.8
c	± 4.0	± 1.0
d	± 2.0	± 2.0
e	± 1.0	± 4.0
f	± 0.8	± 5.0
g	± 0.5	± 8.0

II. CHARACTERISTIC EQUATIONS AND PROPAGATION PROPERTIES OF A GROUNDED SLAB GUIDING STRUCTURE

Fig. 1 shows a schematic illustration of a grounded slab waveguide backed by a perfect electric conductor (PEC). The propagation direction is chosen to be the $+z$ direction, and the slab thickness is h. The relative permittivity and permeability of the slab ($x < h$) are denoted as ε_{r1} and μ_{r1}, respectively. The material parameters in the slab region for this investigation are chosen as listed in Table 1. Each of seven combinations of the material parameters is prepared for both the DPS ($\mu_{r1} > 0$ and $\varepsilon_{r1} > 0$) and the DNG ($\mu_{r1} < 0$ and $\varepsilon_{r1} < 0$) media in order to clarify the roles of the material constants in the guided dispersion characteristics. The product $\mu_{r1}\varepsilon_{r1}$ is invariant as 4.0, *i.e.*, $\mu_{r1}\varepsilon_{r1} = 4.0$, for an identical reference for the dispersion characteristics. The relative permittivity and permeability in the region of ($x > h$) are assumed to be unity, $\varepsilon_{r2} = \mu_{r2} = 1.0$; *i.e.*, they are the same as those of the free space. Because the slab region is denser, *i.e.*, $\mu_{r1}\varepsilon_{r1} > \mu_{r2}\varepsilon_{r2}$, which is a guiding condition for conventional grounded dielectric slab waveguides, parts of the propagation characteris-

Table 2. Characteristic equations of grounded MTM slab waveguides.

	OS mode $(\sqrt{\mu_{r1}\varepsilon_{r1}} > \bar{\beta} > \sqrt{\mu_{r2}\varepsilon_{r2}})$	SP mode $(\bar{\beta} > \sqrt{\mu_{r1}\varepsilon_{r1}} > \sqrt{\mu_{r2}\varepsilon_{r2}})$
	$k_1 = k_0(\mu_{r1}\varepsilon_{r1} - \bar{\beta}^2)^{1/2}$ $k_2 = k_0(\bar{\beta}^2 - \mu_{r2}\varepsilon_{r2})^{1/2}$	$k_1 = k_0(\bar{\beta}^2 - \mu_{r1}\varepsilon_{r1})^{1/2}$ $k_2 = k_0(\bar{\beta}^2 - \mu_{r2}\varepsilon_{r2})^{1/2}$
Antisymmetric TM_m mode $(m = 0,2,4,\cdots)$	$\frac{\varepsilon_{r2}k_1h}{\varepsilon_{r1}k_2h}\tanh(k_1h) - 1 = 0$	$\frac{\varepsilon_{r2}k_1h}{\varepsilon_{r1}k_2h}\tanh(k_1h) + 1 = 0$
Symmetric TE_m mode $(m = 1,3,5,\cdots)$	$\frac{\mu_{r2}k_1h}{\mu_{r1}k_2h}\coth(k_1h) + 1 = 0$	$\frac{\mu_{r2}k_1h}{\mu_{r1}k_2h}\coth(k_1h) + 1 = 0$

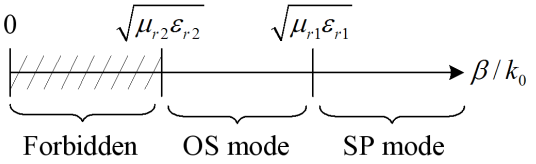

Fig. 2. The OS and the SP mode regions of the normalized propagation constants.

tics are expected to be similar to those of a conventional grounded dielectric slab. For this reason, we limit our attention to this $\mu_{r1}\varepsilon_{r1} > \mu_{r2}\varepsilon_{r2}$ case.

At this point, one might doubt whether negative electric and magnetic energies are physically meaningful or not when frequency-independent materials are used in the calculations with the expression

$$W = \frac{1}{2}(\varepsilon|\vec{E}|^2 + \mu|\vec{H}|^2) \tag{1}$$

where ε and μ are the permittivity and the permeability, respectively ($\varepsilon = \varepsilon_0\varepsilon_r$ and $\mu = \mu_0\mu_r$; here ε_0 and μ_0 are the permittivity and the permeability of free space, respectively.). It has been generally accepted that the negative electric and magnetic energies do not violate universal power conservation and causality [18].

The characteristic equations and their belongings are tabulated in Table 2, which can be readily obtained by the standard steps of a boundary-value problem. $\bar{\beta}(= \beta/k_0)$ is the normalized propagation constant in the $+z$ direction normalized by the free space wave number k_0. $k_i(i = 1, 2)$ is the transverse propagation constant. For our structure, the characteristic equations for the antisymmetric TM and the symmetric TE modes can be obtained. On the other hand, those for the symmetric TM and the antisymmetric TE modes do not exist due to the PEC grounding [19]. There exist two distinct operating modes. One is the ordinary surface (OS) mode, whose characteristic equations are the same as those of the conventional grounded dielectric slabs, along which a surface wave is guidable [19]. The other operating mode is called the surface polariton (SP) mode because the characteristic equations are identical to those for a plasma slab [20] that can support surface (plasmon) polaritons [21, 22]. The existence of surface polaritons at the interface between the LHM material and the conventional dielectric material has already been demonstrated by Ruppin [23,24]. The allowed regions for the existence of both operating modes are shown in Fig. 2 and are associated with the expressions of the transverse propagation constants in Table 2. The normalized propagation constant exceeding $(\mu_{r1}\varepsilon_{r1})^{1/2}$ allows the SP mode to exist. Fig. 3 shows a sketch of the absolute value of the lateral electric field distributions of the OS and the SP modes. The electric field components for the TM and the TE modes are E_z and E_y, respectively. The OS mode can have higher-order modes as the operating frequency and/or slab thickness increases whereas the SP mode has a monomode property due to the non-oscillatory nature of the fields inside the slab region. As Fig. 3 shows, the peaks of the electric field in the OS mode exist within the slab region, but the field (and the power) distributions of the SP mode decay in both regions from the interface between the slab and the free space, *i.e.*, $x = h$. The SP modes are only available for the DNG cases, and they have only principal modes, such as TM_0 and TE_1 modes, due to the non-oscillatory properties of the tanh and the coth functions (see Table 2), which exhibit monomode properties. Detailed descriptions with numerical examples will be given in Section III.

Fig. 4 shows a sketch of the Poynting vectors near the interface between the slab and the free space. The guided wave along the grounded DPS slab is a forward ($+z$-direction) wave because power flow along both regions of the slab and in free space is also forward, as shown in the Fig. 4(a). In the case of the grounded DNG slab waveguides, the power flows in the free space and in the slab regions are forward $+z$ and backward $-z$, respectively. The backward guided wave along the DNG slab region is due to the left-handedness, as mentioned already. This antiparallel power flow in each region forms a vortex-like Poynting vector distribution, as shown in the Fig. 4(b). The source of the backward waves is a portion of the vortex-like behavior of the guided power at the interface between different media [10,25–27]. Sometimes, it can also be viewed as the coupled mode [28]. Since the phase propagation is set to be positive, *i.e.*, $\beta > 0$, the power flow in the slab region should be negative due to the left-handedness of

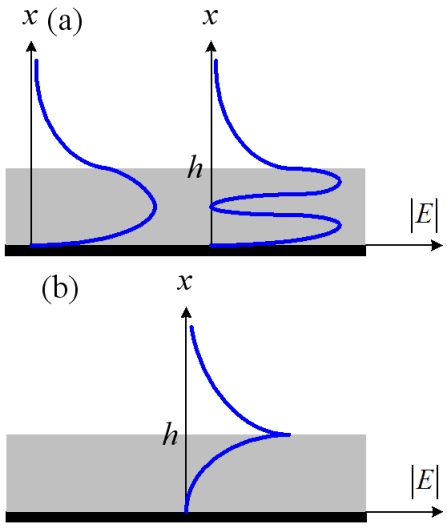

Fig. 3. Sketch of the absolute value of the lateral electric field distributions; (a) the OS mode and (b) the SP mode.

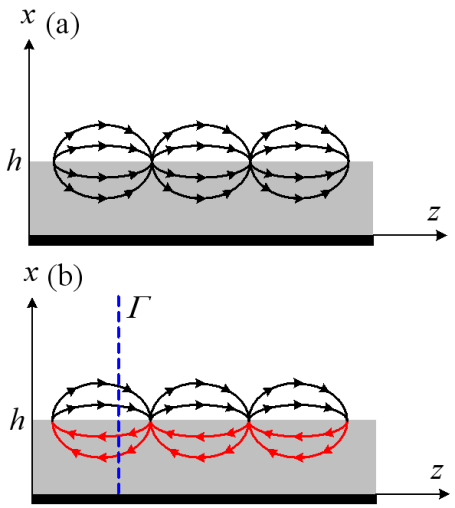

Fig. 4. Sketch of the Poynting vectors near the boundary between the slab and the free space: (a) DPS case and (b) DNG case.

the DNG media. Judgments as to whether the guided wave propagating along the entire cross section of the waveguide, *e.g.*, $\Gamma(0 < x < \infty)$ in the Fig. 4(b), is forward or backward can be done by using the sign of the total power flux density. If $\int_\Gamma (\vec{E} \times \vec{H}) \cdot d\vec{S} > 0 (< 0)$, then the guided wave is forward (backward). In other words, if the forward (backward) wave power in the free space (DNG slab) region is dominant, the total power density becomes positive (negative). This situation can occur not only in the DNG/DPS interface [10,25,26] but also in the SNG[2]/DPS interface [27].

The difference between the negative phase and group velocities with associated situations are illustrated in

[2] Single-negative, *i.e.*, $\varepsilon < 0$ and $\mu > 0$, or $\varepsilon > 0$ and $\mu < 0$.

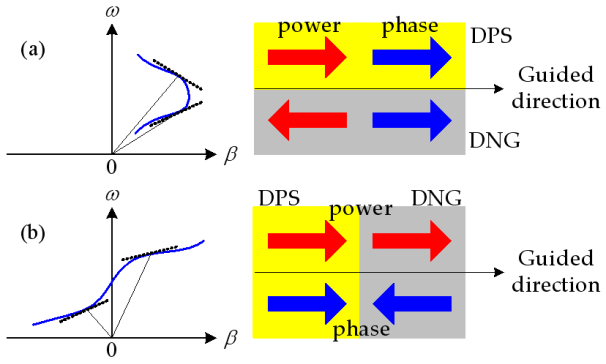

Fig. 5. Two kinds of wave velocities with their corresponding dispersion curves: (a) NGV and (b) NPV. In the dispersion curves, the slopes of the solid and the dotted lines represent the signs of the phase and the group velocities, respectively. Our structure belongs to the NGV case.

Fig. 5; *i.e.*, there are two kinds of negative wave velocities. Fig. 5(a) and (b) describes the NGV and the NPV cases with their dispersion curves and practical situations of wave propagations, respectively. The slopes ω/β(solid line) and $\partial\omega/\partial\beta$ (dotted line) represent the phase and the group velocities [29]. The NGV structure is much more similar to the current structure (grounded slab); *i.e.*, the interface between the two dissimilar media is parallel to the direction of wave propagation. Of course, our structure belongs to the NGV case, *i.e.*, Fig. 5(a), where the phase flows in both regions are positive ($\beta > 0$ and $\omega/\beta > 0$) and the power flows are reversed ($\partial\omega/\partial\beta > 0$ in DPS region and $\partial\omega/\partial\beta < 0$ in DNG region). On the other hand, a representative example of NPV supporting structure is a composite right/left-handed (CRLH) structure [8]. In Fig. 5(b), the directions of the power flows in both regions are positive ($\partial\omega/\partial\beta > 0$), but the phase flows are reversed ($\beta > 0$ in DPS region and $\beta > 0$ in DNG region).

III. NUMERICAL RESULTS AND DISCUSSIONS

1. Antisymmetric TM$_m$ Modes

The characteristic equations in Table 2 are numerically solved by using Newton's method [30], and the eigenmode solution is the normalized propagation constants (β/k_0) with respect to the normalized frequency ($k_0 h$), with which the propagation characteristics of the grounded DPS and DNG slabs will be discussed. Fig. 6 shows the dispersion characteristics of the grounded DPS and DNG slab waveguides for the antisymmetric TM$_m$ mode. As Table 2 shows, the dispersion characteristics of the TM modes are directly associated with the permittivity (in particular, their signs) rather than the permeability. The case of $\varepsilon_{r1} = 4.0$ and $\mu_{r1} = 1.0$ (case *c* in Table 1) for a conventional grounded dielec-

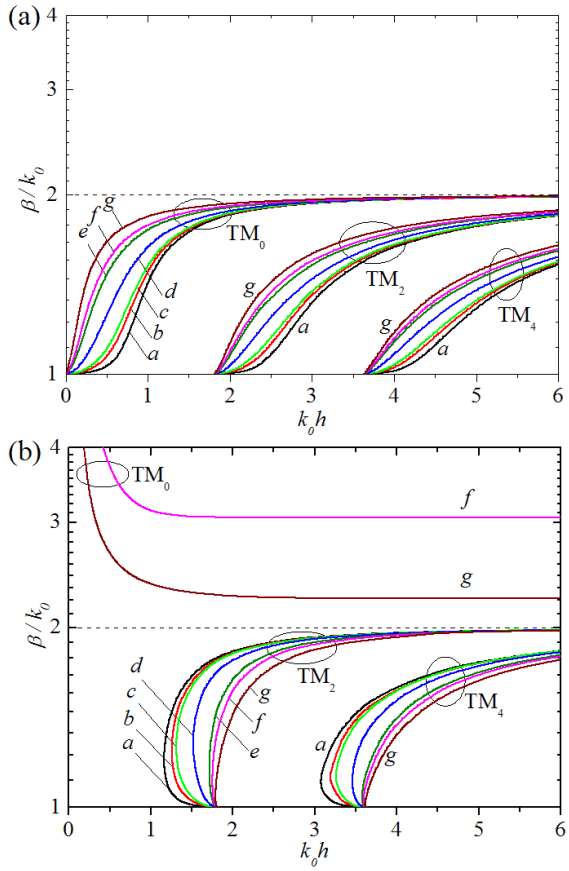

Fig. 6. Dispersion curves of the grounded slab waveguides for the antisymmetric TM_m modes: (a) DPS and (b) DNG slabs. The characters represent the arbitrary media in Table 1.

tric slab waveguide is also included in Fig. 6(a). One of the well-known dispersion characteristics of conventional dielectric slab waveguides is that the cutoff of the principal mode (TM_0 mode) does not exist, which means that the mode can propagate, regardless of how thin the slab thickness is. This absence of a TM_0 mode cutoff is also observed for other DPS combinations, *i.e.*, cases of $\mu_{r1} \neq 1.0$, as shown in Fig. 6(a). While the TM_0 modes for any material combinations of grounded DPS slab waveguides are not suppressed, the TM_0 modes of the DNG cases with $|\varepsilon_{r1}| \geq 1.0$ have all been suppressed, as shown in Fig. 6(b). In contrast, the TM_0 modes with $|\varepsilon_{r1}| < 1.0$, *i.e.*, the f ($\varepsilon_{r1} = -0.8$ and $\mu_{r1} = -5.0$) and the g ($\varepsilon_{r1} = -0.5$ and $\mu_{r1} = -8.0$) cases, can be supported. The guided region for the TM_0 modes with $|\varepsilon_{r1}| < 1.0$ (f and g cases) belongs to the SP mode region ($\beta/k_0 > \mu_{r1}\varepsilon_{r1}$). Also, these TM_0 modes with $|\varepsilon_{r1}| < 1.0$ are all backward waves due to the dispersion curves having negative slopes [11, 17, 26]. As we mentioned in the previous section, this is because that the power propagating along the DNG slab region is greater than that propagating along the free space region, which is also usually observed in plasma waveguides [31,32] or

Table 3. Normalized cutoff frequency of the grounded slab waveguide.

TM_0	TE_1	TM_2	TE_3	TM_4	TE_5
0	0.91	1.82	2.73	3.63	4.54

surface plasmon waveguides [33, 34], even though they do not include a DNG region in their guiding cross sections. (Dispersion curves with positive slopes correspond to forward waves, as expected.)

For lower normalized frequencies, the TM_0 modes with $|\varepsilon_{r1}| < 1.0$ can also support superslow waves [35] whose normalized propagation constants can be very high, exhibiting extremely slow phase velocity because the normalized phase velocity is the reciprocal of the normalized propagation constants, *i.e.*, $v_p/c = k_0/\beta$, where c is the speed of light. The electromagnetic waves corresponding to superslow waves can also propagate along very thin slabs. This represents the possibility of subwavelength guidance, which can be of significant utility in near-field optics applications [36,37] and in designs of compact electromagnetic devices [38, 39]. Furthermore, relatively higher values of the normalized propagation constants (superslow waves) are favorable from the viewpoint of tighter power confinement within or near the slab regions whereas power confinements for the DPS counterpart are poor due to the lower value of the normalized propagation constants, which is limited under the condition of $\beta/k_0 < \sqrt{\mu_{r1}\varepsilon_{r1}}$. (A unity value of the normalized propagation constant reflects the propagation in the guided wave being essentially identical to that in free space, *i.e.*, $\beta = k_0$. Thus, the lateral extent ($+x$-direction in Fig. 1) of the power carried by the guided wave for $\beta = k_0$, which is nearly the same as the plane electromagnetic wave case, is absolutely more stretched than that of the power for $\beta > k_0$, which is actually guided. This means that higher normalized propagation constants are directly associated with tighter power confinements of the guided waves near the slab region of the guide.) The modes with higher normalized propagation constants may have an advantage in reducing unnecessary coupling of electromagnetic energy into adjacent circuits. Of course, the normalized cutoff frequency of the TM_0 mode for the DNG case does not exist, either.

The guided dispersion characteristics of higher-order modes are also shown in Fig. 6. The normalized cutoff frequencies of higher order modes are shown in the Table 3. The normalized cutoff frequency for both the DPS and the DNG cases does not change for various combinations of both material parameters, once their product, for example, $\mu_{r1}\varepsilon_{r1} = 4.0$ here, is kept constant. In the DPS case, the cutoff frequency is the lowest frequency of guided propagation at which $\beta/k_0 = 1.0$, and it did not change for various combinations of the material parameters as long as the product $\mu_{r1}\varepsilon_{r1}$ was kept constant. In contrast, the lowest frequency of propagation for the DNG case is the bifurcation frequency point, where the

onset of forward (with a positive slope in the dispersion curve) and backward (with negative slope) waves occurs, not the frequency for $\beta/k_0 = 1.0$, as shown in Fig. 6(b). The coexistence of forward and backward waves in the frequency range between the bifurcation frequency and the frequency for $\beta/k_0 = 1.0$ is the significant difference between the dispersion characteristics of DPS and DNG waveguides. However, this bifurcation frequency point changes for various combinations of the material parameters, as shown in Fig. 6(b). In order to maintain consistency between the mode designations of the DPS and the DNG cases, the cutoff frequency concept of the DNG waveguide defined as the frequency for $\beta/k_0 = 1.0$ is very useful because the cutoff frequency, *i.e.*, the frequency at which, $\beta/k_0 = 1.0$ is constant when the product $\mu_{r1}\varepsilon_{r1}$ of any combinations of material parameters, whether they are DPS or DNG materials, is constant. For the classifications of the DNG waveguide modes, which are relatively unknown, the mode designations of the well-known DPS waveguide can be directly applied to those of the DNG waveguide because the cutoff frequencies defined as above for both the DPS and the DNG cases are identical. For this reason, the cutoff frequencies of the DNG waveguide in this paper have been chosen to be same as those for the DPS case.

For higher-order modes, the normalized propagation constants of the DPS and the DNG cases cannot exceed the limit of $(\mu_{r1}\varepsilon_{r1})^{1/2} = 2.0$, but approach it as the normalized frequency increases, which is the upper limit of the OS mode as shown in Fig. 2. In other words, higher-order TM modes of grounded DNG slabs all belong to the OS mode whereas the principal TM mode can have SP mode solutions when $\varepsilon_{r1} < 1.0$. DPS slabs with higher values of the relative permittivity have lower values of the normalized propagation constants and exhibit less power confinement within or near the slab region. In contrast to the DPS cases, DNG slabs with higher relative permittivity exhibit higher normalized propagation constants in their forward wave portions in the dispersion curves. In this sense, the power confinement characteristics for grounded DPS slabs are opposite those for grounded DNG slabs, even though the product of the permittivity and the permeability is the same. The forward and the backward waves with respective positive and negative slopes always exist simultaneously for the higher-order modes of grounded DNG slabs, which might be potentially applied to some switching devices. This is due to the existence of backward wave power propagation (NGV case), which is one of the inherent properties of DNG materials. The spectral ranges of the coexistence are reduced with increasing absolute value of the relative permittivity.

2. Symmetric TE$_m$ Modes

Fig. 7 shows the dispersion curves of the grounded DPS and DNG slab waveguides for symmetric TEm modes. For the TE modes, as shown in the Table 2, the dispersion characteristics are mainly influenced by the permeability rather than the permittivity of the media. (For the TM modes, discussions on the extraordinary guided dispersions of grounded DNG slabs have been given with the permittivities in previous subsections.) Unlike the previous TM mode case, the principal TE mode (TE$_1$ mode) of the grounded DPS slab waveguide has a cutoff frequency, so it cannot propagate below the normalized cutoff frequency. If the DPS slabs are replaced by DNG slabs, however, the TE$_1$ mode can propagate over the cutoff frequency region, *i.e.*, $0 < k_0h < 0.91$, as shown in Fig. 7(b). Whereas the antisymmetric TM$_1$ modes with $|\varepsilon_{r1}| \geq 1.0$ were all suppressed as shown in Fig. 6, none of symmetric TE$_1$ modes were suppressed. Only backward waves exist if the absolute value of the relative permittivity is greater than unity, *i.e.*, $|\mu_{r1}| \geq 1.0$. Alù *et al.* also considered the DNG slab waveguide with $|\mu_{r1}| \geq 1.0$, based upon their observation that the TE$_1$ mode can support higher values of the normalized propagation constants even in very thin slabs [40]. However, they did not consider the case of $|\mu_{r1}| < 1.0$, which will provide another possibility for device application. If $|\mu_{r1}| < 1.0$, the TE$_1$ mode has

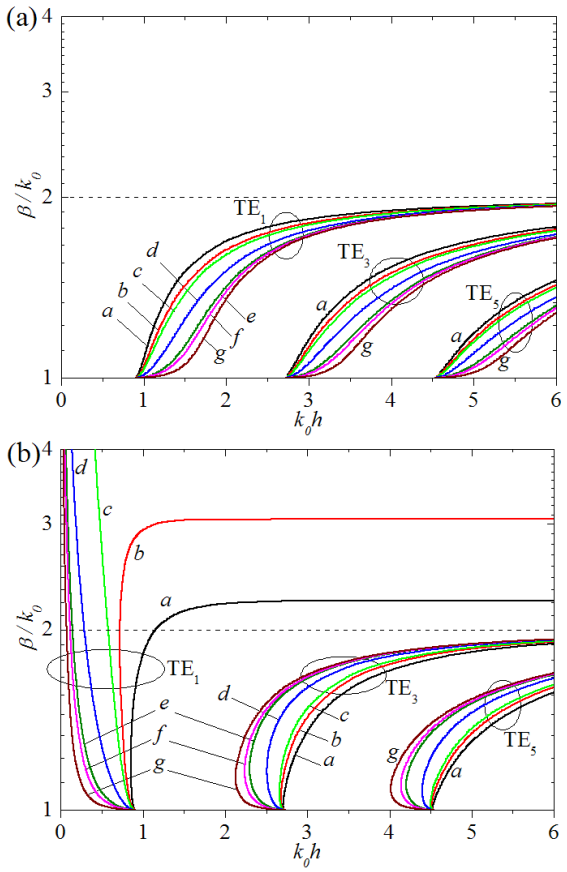

Fig. 7. Dispersion curves of the grounded slab waveguides for the symmetric TE$_m$ modes: (a) DPS and (b) DNG slabs. The characters represent the arbitrary media in Table 1.

forward SP modes, which cannot be obtained in conventional grounded DPS slab waveguides. This forward SP mode is much favored over the OS mode from the viewpoint of enhanced power confinement and a wide, flat operating region. The dispersion curves of the OS and the SP modes in Fig. 7(b) are smoothly continued at the border between them, *i.e.*, at $\bar{\beta} = 2.0$ (represented by the dashed lines), while the OS and the SP modes are entirely isolated in the cases of the previous antisymmetric TM modes, as shown in Fig. 6(b). From this results, we can see that the dispersion characteristics become quite different, depending on whether $|\mu_{r1}| \geq 1.0$ or $|\mu_{r1}| < 1.0$.

In Fig. 7(a), for the DPS cases, the modes with higher relative permeabilities have higher normalized propagation constants (meaning more enhanced power confinement), similar to the previous case of the antisymmetric TM_m mode. The cutoff frequency of each higher order mode is also invariant with respect to variations in the material parameters. In more detail, the TE_3 and the TE_5 modes for the DNG cases have the same cutoff frequencies as those in the DPS cases, as listed in Table 3. The dispersion characteristics of the higher-order TE modes are similar to those of the previous TM modes. The higher-order mode for the DNG cases cannot have a SP mode solution and always has forward and backward waves in the OS mode region. Also, a higher normalized propagation constant is obtained for a relative larger permeability. The spectral range for the coexistence of forward and backward waves is reduced as the relative permeability decreases, which is identical to the tendency observed in the previous antisymmetric TM mode cases.

IV. CONCLUSIONS

The guided dispersion characteristics of grounded DNG slab waveguides are numerically investigated for various material constants. Comparisons of the dispersion characteristics between the grounded DNG slab waveguide and the DPS counterpart are also made in detail. For an identical reference, all the calculations are done with the product of the two material parameters (relative permittivity and the relative permeability) kept invariant at $\mu_{r1}\varepsilon_{r1} = 4.0$. As expected, antisymmetric TM and symmetric TE modes can propagate whereas symmetric TM and antisymmetric TE modes cannot exist due to the PEC ground. Interestingly, it is observed that, for the antisymmetric TM_m mode, the TM_0 modes with $|\varepsilon_{r1}| < 1.0$ support backward waves and the modes with $|\varepsilon_{r1}| \geq 1.0$ are all suppressed. The guided region for the TM_0 mode belongs to only the SP mode region whereas the higher order-modes exist in the OS mode regions. For the symmetric TEm mode, the principal modes of any material combination are not suppressed. When $|\mu_{r1}| < 1.0$, the principal modes can have forward waves as well as backward waves. In contrast, the TE_1 modes with $|\mu_{r1}| \geq 1.0$ have only backward waves. For any material combinations, the dispersion curves of the TE_1 modes are smoothly continued from the OS to the SP modes (or vice versa) without any seam at their borders, even though they are governed by different characteristic equations. The cutoff frequencies do not change even when the material parameters are changed, provided the product of the permittivity and the permeability is kept the same. Forward and backward waves always exist simultaneously for higher-order modes of grounded DNG slabs. The power confinement characteristics of grounded DPS and DNG slab waveguides are reversed. The spectral region for coexistence of both forward and backward waves is found only for grounded DNG slab waveguides, and their properties with respect to the material constants are discussed. The TM_0 modes with $|\varepsilon_{r1}| < 1.0$ and the TE_1 modes with $|\mu_{r1}| \geq 1.0$ of grounded DNG slab waveguides may find applications in areas of the subwavelength compact waveguiding structures with the enhanced power-confinement characteristics of the superslow waves. The present result is restricted to the case of $\mu_{r1}\varepsilon_{r1} = 4.0$ as a representative example of $\mu_{r1}\varepsilon_{r1} > 1.0$. The guided dispersion characteristics for the case of $0 < \mu_{r1}\varepsilon_{r1} < 1.0$ [14,16] remains to be investigated further for completeness of the discussion of the roles of the material parameters in determining the guided dispersion characteristics.

ACKNOWLEDGMENTS

This work was supported by grant No. R01-2004-000-10158-0 from the Basic Research Program of the Korea Science & Engineering Foundation.

REFERENCES

[1] R. E. Collin, *Field Theory of Guided Waves*, 2nd ed. (IEEE Press, New York, 1991), Chap. 12.

[2] I. J. Bahl and P. Bhartia, IEEE Trans. Microwave Theory Tech. **28**, 1205 (1980); I. J. Bahl and K. C. Gupta, IEEE Trans. Antennas Propag. **24**, 73 (1976); I. J. Bahl and K. C. Gupta, IEEE Trans. Antennas Propag. **23**, 584 (1975); I. J. Bahl and K. C. Gupta, IEEE Trans. Antennas Propag. **22**, 119 (1974).

[3] J. B. Pendry, A. J. Holden, W. J. Stewart and I. Young, Phys. Rev. Lett. **76**, 4773 (1996); J. B. Pendry, A. J. Holden, D. J. Robbins and W. J. Stewart, J. Phys.: Condens. Matter **10**, 4785 (1998).

[4] J. B. Pendry, A. J. Holden D. J. Robbins and W. J. Stewart, IEEE Trans. Microwave Theory Tech. **47**, 2075 (1999).

[5] D. R. Smith, W. J. Padilla, D. C. Vier, S. C. Nemat-Nasser and S. Schultz, Phys. Rev. Lett. **84**, 4184 (2000).

[6] V. G. Veselago, Sov. Phys. Usp. **10**, 509 (1968).

[7] A. D. Boardman, N. King and L. Velasco, Electromagnetics **25**, 365 (2005); M. Perrin, S. Fasquel, T. Decoopman, X. Mélique, O. Vanbésien, E. Lheyrette and D. Lippens, J. Opt. A: Pure Appl. Opt. **7**, S3 (2005); Z. Ye, Chinese J. Phys. **43**, 1 (2005); N. Engheta and R. W. Ziolkowski, IEEE Trans. Microwave Theory Tech. **53**, 1535 (2005); S. A. Ramakrishna, Rep. Prog. Phys. **68**, 449 (2005); J. B. Pendry, Contemporary Phys. **45**, 191 (2004); D. R. Smith, J. B. Pendry and M. C. Wiltshire, Science **305**, 788 (2004); K. Yu. Bliokh and Yu. P. Bliokh, Phys. Usp. **47**, 393 (2004).
[8] C. Caloz and T. Itoh, Proc. IEEE **93**, 1744 (2005); A. Lai, C. Caloz and T. Itoh, IEEE Microwave Mag. **5**, 34 (2004).
[9] S. A. Darmanyan, M. Nevière and A. A. Zakhidov, Opt. Commun. **225**, 233 (2003).
[10] Y. He, Z. Cao and Q. Shen, Opt. Commun. **245**, 125 (2005).
[11] I. V. Shadrivov, A. A. Sukhorukov and Y. S. Kivshar, Phys. Rev. E **67**, 057602 (2003).
[12] B.-I. Wu, T. M. Grzegorczyk, Y. Zhang and J. A. Kong, J. Appl. Phys. **93**, 9386 (2003).
[13] H. Cory and A. Barger, Microwave Opt. Tech. Lett. **38**, 392 (2003).
[14] P. Baccarelli, P. Burghignoli, G. Lovat and S. Paulotto, IEEE Antennas Wireless Propag. Lett. **2**, 269 (2003).
[15] P. Baccarelli, P. Burghignoli, F. Frezza, A. Galli, P. Lampariello, G. Lovat and S. Paulotto, IEEE Trans. Microwave Theory Tech. **53**, 1431 (2005).
[16] C. Li, Q. Sui and F. Li, Prog. Electromagnetic Res. **51**, 187 (2005).
[17] S. F. Mahmoud and A. J. Viitanen, Prog. Electromagnetic Res. **51**, 127 (2005).
[18] R. W. Ziolkowski and A. D. Kipple, IEEE Trans. Antennas Propag. **51**, 2626 (2003); R. W. Ziolkowski and E. Heyman, Phys. Rev. E **64**, 056625 (2001); R. W. Ziolkowski, Phys. Rev. E **63**, 046604 (2001).
[19] D. M. Pozar, *Microwave Engineering*, 2nd ed. (John Wiley & Sons, Inc., New York, 1998), Chap. 3.
[20] Yu. M. Aliev, H. Schluter and A. Shivariva, *Guided-Wave-Produced Plasmas* (Springer-Verlag, Berlin, 2000), Chap. 3.
[21] V. M. Agrannovich and D. L. Mills, *Surface Polaritons: Electromagnetic Waves at Surfaces and Interfaces* (North-Holland Publishing Company, New York, 1982).
[22] A. D. Boardman, *Electromagnetic Surface Modes* (John Wiley & Sons, Ltd., New York, 1982).
[23] R. Ruppin, Phys. Lett. A **277**, 61 (2000).
[24] R. Ruppin, J. Phys.: Condens. Matter **13**, 1811 (2001).
[25] J. Schelleng, C. Monzon, P. F. Loschialpo, D. W. Forester and L. N. Medgyesi-Mitschang, Phys. Rev. E **70**, 066606 (2004).
[26] J. He and S. He, IEEE Microwave Wireless Comp. Lett. **16**, 96 (2006).
[27] J. Nkoma, R. Loudon and D. R. Tilley, J. Phys. C: Solid State Phys. **7**, 3547 (1974).
[28] J. R. Pierce, *Almost All About Waves* (The MIT Press, Cambridge, 1974), Chap. 7.
[29] S. Ramo, J. R. Whinnery and T. V. Duzer, *Fields and Waves in Communication Electronics*, 3rd ed. (John Wiley & Sons, Inc., New York, 1993), Chap. 5.
[30] MATHEMATICA ver. 4.0 (Wolfram Research, Inc.).
[31] A. A. Oliner and T. Tamir, J. Appl. Phys. **33**, 231 (1962).
[32] V. L. Granatstein, S. P. Schlesinger and A. Vigants, IEEE Trans. Antennas Propag. **11**, 489 (1963).
[33] H. Khosravi, D. R. Tilley and R. Loudon, J. Opt. Soc. Am. A **8**, 112 (1991).
[34] P. Tournois and V. Laude, Opt. Commun. **137**, 41 (1997).
[35] I. S. Nefedov and S. A. Tretyakov, Radio Sci. **38**, RS1101 (2003).
[36] S. S. Choi. J. T. Ok, D. W. Kim, M. Y. Jung and M. J. Park, J. Korean Phys. Soc. **45**, 1659 (2004).
[37] S. S. Choi, D. W. Kim and M. J. Park, J. Korean Phys. Soc. **45**, 1500 (2004).
[38] S. Lee, J. Korean Phys. Soc. **43**, 507 (2004).
[39] S. K. Kim and H. R. Fetterman, J. Korean Phys. Soc. **42**, L305 (2003).
[40] A. Alù and N. Engheta, in *Negative Refraction Metamaterials: Fundamental Properties and Applications*, edited by G. V. Eleftheriades and K. G. Balmain, (John Wiley & Sons, Inc., New York, 2005), p. 339.